Journal of Sound and Vibration (1998) **218**(1), 45–63
Article No. sv981779

A STRUCTURAL FLEXIBILITY TRANSFORMATION MATRIX FOR MODELLING OPEN-KINEMATIC CHAINS WITH REVOLUTE AND PRISMATIC JOINTS

N. G. Chalhoub and L. Chen

Department of Mechanical Engineering, *Wayne State University*, *Detroit*, *MI* 48202, *U.S.A.*

(*Received* 1 *August* 1997, *and in final form* 1 *June* 1998)

A general approach to systematically derive the equations of motion of flexible open-kinematic chains is presented in this paper. The methodology exploits the serial characteristic of the kinematic chain by complementing the 4×4 Denavit–Hartenberg transformation matrix with a 4×4 structural flexibility matrix. The latter is defined based on a floating coordinate system which rendered the formulation applicable to both prismatic and revolute joints. The versatility of the approach is demonstrated through its implementation to formulate forward kinematic problems of manipulators with revolute and prismatic joints. Moreover, the proposed flexibility matrix is used in the development of a dynamic model for a compliant spherical robotic manipulator. This task has a dual purpose. First, it demonstrates how the flexibility matrix can be implemented in a systematic approach for deriving the equations of motion of an open-kinematic chain that account for the axial geometric shortening, the torsional vibration, and the in-plane and out-of-plane transverse deformations of the compliant member. Second, the inclusion of the torsional vibration in the equations of motion serves to broaden the scope of previous research work done on modelling open-kinematic chains. The formulation can now address dynamic problems that are not limited to the positioning but are also concerned with the orientation of rigid body payloads as they are being manipulated by robotic manipulators. The digital simulation results exhibit the interaction between the torsional vibration and the rigid body motion of the arm. Furthermore, they demonstrate a strong coupling effect between the torsional vibration and the transverse deformations of the arm whenever the payload is not grasped at its mass center by the gripper.

1. INTRODUCTION

Many models have been developed to predict the rigid and flexible motions of open-kinematic chains by using the general vector-dyadic formulation [1–3]. The conceptual framework of this method does not exploit the inherent characteristics of kinematic chains in order to simplify the derivation of the equations of motion.

Sunada and Dubowsky [4] have used the 4×4 Denavit–Hartenberg (D–H) homogeneous transformation matrix [5] along with the Lagrange principle to derive the equations of motion of flexible manipulators that are made of irregular

0022–460X/98/460045 + 19 $30.00/0

shaped links. The flexible motion was treated as deviations from the nominal rigid body motion of the linkage. Furthermore, the kinematics of the ith link were assumed to be unaffected by the deformations of the superseding links in the chain.

Book [6] introduced a 4×4 structural flexibility matrix to be used along with the D–H transformation matrix to provide a conceptually straightforward approach for modelling flexible manipulators. The methodology requires two co-ordinate systems to be assigned at the end-points of each compliant link. The deformations at the distal end of the member are represented by defining the origin and orientation of the distal co-ordinate system with respect to the D–H frame. This approach considers the interaction between the rigid and flexible motions and do not assume a nominal rigid body motion of the manipulator. However, the usage of a body fixed co-ordinate system has limited the application of this technique to articulated manipulators. Similar approaches have also been implemented by Judd and Falkenburg [7], Matsuno and Sakawa [8] and Li and Sankar [9].

To render the methodology applicable to flexible kinematic chains with prismatic joints, the current formulation implements a 4×4 structural flexibility matrix that is derived based on a floating co-ordinate system [10]. The flexibility matrix describes the general deformations at an arbitrary point on the neutral axis of the beam. It considers the longitudinal, torsional, in-plane and out-of-plane transverse deformations along with the effects of rotary inertia, shear deformation and axial geometric shortening.

The versatility of the current structural flexibility matrix is demonstrated through its implementation to formulate forward kinematic problems of manipulators with revolute and prismatic joints. Furthermore, the proposed flexibility matrix is used in the development of a dynamic model for a compliant spherical robotic manipulator. This step has a dual purpose. First, it demonstrates how the flexibility matrix can be implemented in a systematic approach for deriving the equations of motion of an open-kinematic chain that take into consideration the axial geometric shortening, the torsional vibration, the in-plane and out-of-plane transverse deformations of the compliant link. Second, the inclusion of the torsional vibration in the equations of motion serves to broaden the scope of previous research work done in the area of modelling open-kinematic chains. The formulation can now address dynamic problems that are not limited to the positioning but also concerned with the orientation of rigid body payloads as they are being manipulated by robotic manipulators.

It should be mentioned that most of the available literature have focused on the interaction between the rigid body motion and the in-plane and out-of-plane transverse deformations of the links [1, 2, 11–15]. As a result, most of these studies are limited in their scope of applications to point mass payloads.

Sakawa and Luo [16] have developed a model for a single rotating beam that considers the first two elastic modes for each of the torsional and transverse deformations of the beam. In addition, a rigid body payload is attached, at its mass center, to the free-end of the rotating beam. As a consequence, the torsional and transverse deformations became uncoupled. Moreover, the stiffening effect, induced by the centripetal acceleration, has also been ignored in the formulation.

In general, the gripper of the robot arm grasps the payload by one of its extremities. Holding the manipulated object at a different point than its mass center will subject the robotic manipulator to torques whose magnitudes vary with the robot arm configuration and operating speed. These undesirable torques tend to induce torsional vibrations in the arm which can directly affect the orientation of the manipulated objects. Therefore, the torsional vibrations can no longer be ignored in the equations of motion of robotic manipulators which are intended to perform accurate maneuvers of objects in space.

In this paper, the procedure for constructing a 4×4 structural flexibility matrix, based on a floating co-ordinate system, is presented in section 2. Subsequently, the flexibility matrix is implemented to formulate forward kinematic problems of manipulators with revolute and prismatic joints. In section 4, the dynamic model for a spherical robot arm, which considers the torsional and transverse deformations of the robotic manipulator, is derived in detail. The digital simulation results, presented in section 5, exhibit the arm responses during point-to-point (PTP) maneuvers. They illustrate the relationships with which the rigid body motion and the transverse deformations would interact with the torsional vibrations of the manipulator. Finally, the work is summarized and the main contributions are highlighted.

2. DERIVATION OF THE STRUCTURAL FLEXIBILITY TRANSFORMATION MATRIX

The formulation of the 4×4 structural flexibility transformation matrix, currently available in the literature, is restricted in its application to revolute joints. The objective herein is to build on previous work to generalize the structural flexibility matrix so that it can be applied to deformable beams that are connected to either revolute or prismatic joints.

A general deformation of a beam may involve torsional, axial, in-plane and out-of-plane transverse deflections. Furthermore, the prismatic joint brings about the possibility of having a beam length to thickness ratio of less than 10 (thick beam). Therefore, the rotary inertia and shear deformation effects have to be included in the formulation of the structural flexibility matrix [17]. Moreover, the axial geometric shortening effect is introduced in the current formulation to represent the axial displacement undergone by any point on the compliant link due to bending.

A 3-D elastic body, depicted in Figure 1, is used in the development of the general form for the structural flexibility transformation matrix. A point O_0, belonging to both deformed and undeformed configurations of the body, is assumed to be fixed in space. An inertial coordinate system, $\{x_0, y_0, z_0\}$, is attached at O_0. Furthermore, a floating frame, $\{x_1', y_1', z_1'\}$, is considered to be fixed at point O_1' in the undeformed configuration of the elastic body. As the structure deforms, O_1' takes up a new location at O_1 and $\{x_1', y_1', z_1'\}$ adopts a new orientation defined by $\{x_1, y_1, z_1\}$. The deformations of the body at O_1 are captured by the position vector locating O_1 with respect to O_1'. The slopes of the beam, incurred by its elastic

deformations, are accounted for in the rotation matrix describing the orientation of $\{x_1, y_1, z_1\}$ with respect to $\{x_1', y_1', z_1'\}$.

Therefore, the problem of determining the deformations of the body at O_1 becomes a one of formulating a 4×4 transformation matrix that defines the location and orientation of $\{x_1, y_1, z_1\}$ with respect to $\{x_1', y_1', z_1'\}$. This is done by adopting the partitioned form of the 4×4 D–H transformation matrix

$$T_{1'}^{1} = \begin{bmatrix} R_{1'}^{1} & | & \mathbf{D}_{1'}^{1} \\ \text{---} & | & \text{---} \\ O_{1\times 3} & | & 1 \end{bmatrix}, \tag{1}$$

where $R_{1'}^{1}$ is formulated based on a set of Euler angles to uniquely describe the orientation of $\{1\}$ with respect to $\{1'\}$. The first Euler angular displacement consists of rotating $\{x_1', y_1', z_1'\}$ by α_1 around the z_1'-axis to obtain a new set of co-ordinates $\{x', y', z'\}$. During the second angular displacement, the newly formed co-ordinate system is rotated by α_2 around the y'-axis to get $\{x'', y'', z''\}$. The last angular displacement is responsible for rotating $\{x'', y'', z''\}$ by α_3 around the x''-axis to obtain $\{x_1, y_1, z_1\}$. For large deformations, $R_{1'}^{1}$ is derived by treating the angular displacements α_1, α_2 and α_3 as finite rotations. Therefore, through sequential transformations, $R_{1'}^{1}$ can be written as

$$R_{1'}^{1} = R_{1'}^{(x',y',z')} R_{(x',y',z')}^{(x'',y'',z'')} R_{(x'',y'',z'')}^{1}$$

$$= \begin{bmatrix} c\alpha_1 c\alpha_2 & c\alpha_1 s\alpha_2 s\alpha_3 - s\alpha_1 c\alpha_3 & c\alpha_1 s\alpha_2 c\alpha_3 + s\alpha_1 s\alpha_3 \\ s\alpha_1 c\alpha_2 & s\alpha_1 s\alpha_2 s\alpha_3 + c\alpha_1 c\alpha_3 & s\alpha_1 s\alpha_2 c\alpha_3 - c\alpha_1 s\alpha_3 \\ -s\alpha_2 & c\alpha_2 s\alpha_3 & c\alpha_2 c\alpha_3 \end{bmatrix}. \tag{2}$$

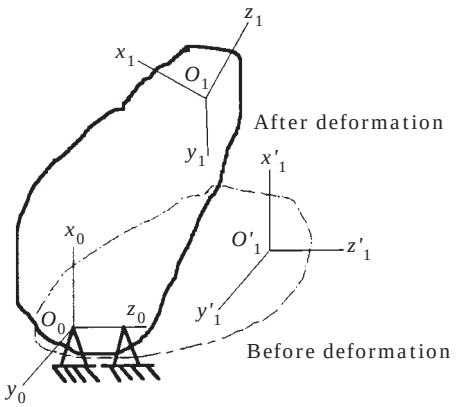

Figure 1. A three-dimensional schematic of a body undergoing a general deformation.

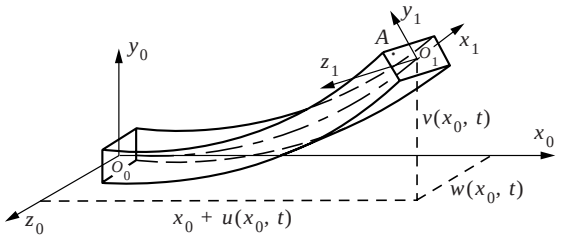

Figure 2. A clamped–free beam undergoing a general deformation.

However, for small deformations, the rotations can be assumed to be infinitesimal. Consequently, $R_{1'}^{1}$ is reduced to

$$R_{1'}^{1} = \begin{bmatrix} 1 & -\alpha_1 & \alpha_2 \\ \alpha_1 & 1 & -\alpha_3 \\ -\alpha_2 & \alpha_3 & 1 \end{bmatrix}. \tag{3}$$

Assuming small deformations, the structural flexibility transformation matrix for a 3-D elastic body can be expressed as

$$T_0^1 = T_0^{1'} T_{1'}^{1} = \left[\begin{array}{c|c} R_0^{1'} & \mathbf{D}_0^{1'} \\ \hline O_{1\times 3} & 1 \end{array}\right]\left[\begin{array}{c|c} R_{1'}^{1} & \mathbf{D}_{1'}^{1} \\ \hline O_{1\times 3} & 1 \end{array}\right]. \tag{4}$$

Note that $R_0^{1'}$ is a constant matrix. Furthermore, without loss of generality, $\{x_0, y_0, z_0\}$ and $\{x_1', y_1', z_1'\}$ co-ordinates can be selected to have the same orientation in space. Thus, $R_0^{1'} = I_{3\times 3}$, which yields the following general form for the structural flexibility matrix:

$$T_0^1 = \left[\begin{array}{c|c} & x_0 \\ I_{3\times 3} & y_0 \\ & z_0 \\ \hline O_{1\times 3} & 1 \end{array}\right]\left[\begin{array}{ccc|c} 1 & -\alpha_1 & \alpha_2 & u \\ \alpha_1 & 1 & -\alpha_3 & v \\ -\alpha_2 & \alpha_3 & 1 & w \\ \hline 0 & 0 & 0 & 1 \end{array}\right]$$

$$= \begin{bmatrix} 1 & -\alpha_1 & \alpha_2 & x_0 + u \\ \alpha_1 & 1 & -\alpha_3 & y_0 + v \\ -\alpha_2 & \alpha_3 & 1 & z_0 + w \\ 0 & 0 & 0 & 1 \end{bmatrix}. \tag{5}$$

For the special case of a beam-like structure, depicted in Figure 2, α_1, α_2 and α_3 correspond to ψ_{y_0}, $-\psi_{z_0}$ and ψ_{x_0}, respectively. Note that ψ_{x_0} represents the torsional vibration of the beam. Whereas, ψ_{y_0} and ψ_{z_0}, which are induced by

shearing and bending deformations, are expressed as $v_{,x_0} - \gamma_{xy_0}$ and $w_{,x_0} - \gamma_{xz_0}$, respectively. By considering the small deformations assumption, the flexibility matrix becomes

$$T_0^1 = \left[\begin{array}{ccc|c} 1 & -\psi_{y_0} & -\psi_{z_0} & x_0 + u \\ \psi_{y_0} & 1 & -\psi_{x_0} & v \\ \psi_{z_0} & \psi_{x_0} & 1 & w \\ \hline 0 & 0 & 0 & 1 \end{array}\right]. \tag{6}$$

Note that the axial deformation, u, consists of the following two components:

$$u = u_l + u_a = u_l - \frac{1}{2}\int_0^{x_0} \left\{\left(\frac{\partial v(\mu, t)}{\partial \mu}\right)^2 + \left(\frac{\partial w(\mu, t)}{\partial \mu}\right)^2\right\} \mathrm{d}\mu, \tag{7}$$

where u_l is the longitudinal deformation and u_a represents the axial geometric shortening undergone by the beam due to its transverse deformations.

The augmented position vector of an arbitrary point A, on the cross-section of the beam that passes through O_1, can be systematically determined from

$$\{\mathbf{r}_A^{\{0\}^T}|1\}^T = T_0^1\{\mathbf{r}_A^{\{1\}^T}|1\}^T = T_0^1\{0 \quad y_1 \quad z_1 \quad | \quad 1\}^T. \tag{8}$$

Note that $y_1 = y_0$ and $z_1 = z_0$ if the Poisson's ratios are ignored.

3. IMPLEMENTATION OF THE STRUCTURAL FLEXIBILITY TRANSFORMATION MATRIX

The versatility of the proposed structural flexibility matrix is demonstrated through its implementation to formulate forward kinematic problems of kinematic chains with revolute and prismatic joints.

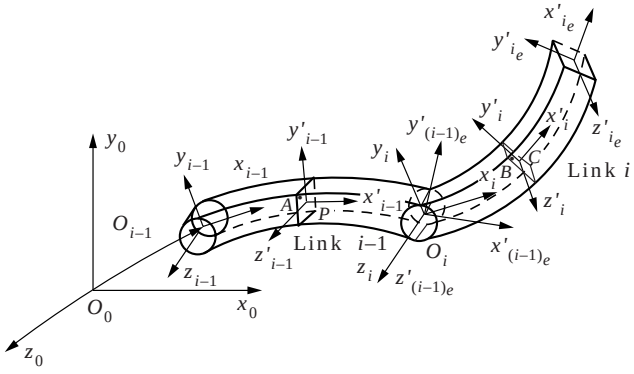

Figure 3. Articulated open-kinematic chain.

3.1. CASE I: KINEMATICS OF TWO FLEXIBLE LINKS CONNECTED TO REVOLUTE JOINTS

Consider the $(i-1)$th and ith members of an articulated multi-link chain (see Figure 3). Only the in-plane and out-of-plane transverse deformations along with their axial geometric shortening effects are included herein. A local co-ordinate system $\{x'_{i-1}, y'_{i-1}, z'_{i-1}\}$ is attached to an arbitrary point P on the neutral axis of the $(i-1)$th link. The structural flexibility matrix, $T_{i-1}^{(i-1)'}$, can be directly obtained from equation (6) by deleting the terms corresponding to torsional and longitudinal vibrations. It can be written as

$$T_{i-1}^{(i-1)'} = \begin{bmatrix} 1 & -\psi_{y_{i-1}} & -\psi_{z_{i-1}} & | & x_{i-1} + u_{a_{i-1}} \\ \psi_{y_{i-1}} & 1 & 0 & | & v_{i-1} \\ \psi_{z_{i-1}} & 0 & 1 & | & w_{i-1} \\ -- & -- & -- & - & --- \\ 0 & 0 & 0 & | & 1 \end{bmatrix}. \tag{9}$$

For an Euler–Bernoulli beam, the total rotations of the local co-ordinate $\{x'_{i-1}, y'_{i-1}, z'_{i-1}\}$ are induced by bending only. As a consequence, the expressions for $\psi_{y_{i-1}}$ and $\psi_{z_{i-1}}$ will be reduced to $v_{i-1,x_{i-1}}$ and $w_{i-1,x_{i-1}}$, respectively.

The augmented position vector of any point A, located on the cross-section of the $(i-1)$th beam that passes through point P, can be obtained from

$$\{\mathbf{r}_A^{\{0\}^T}|1\}^T = T_0^{i-1} T_{i-1}^{(i-1)'} \{\mathbf{r}_A^{\{i-1\}'^T}|1\}^T = T_0^{i-1} T_{i-1}^{(i-1)'} \{0 \quad y'_{i-1} \quad z'_{i-1} \quad | \quad 1\}^T. \tag{10}$$

Similar reasoning is followed to determine the position vector of an arbitrary point on the ith link. First, define $\{x'_{(i-1)_e}, y'_{(i-1)_e}, z'_{(i-1)_e}\}$ to be $\{x'_{i-1}, y'_{i-1}, z'_{i-1}\}$ when its origin coincides with the distal end-point O_i on the neutral axis of the $(i-1)$th link. Then, the rigid body motion of the ith link, relative to the $(i-1)$th link, can be accounted for by introducing a new frame, $\{i\}$. The latter is assigned by rotating $\{x'_{(i-1)_e}, y'_{(i-1)_e}, z'_{(i-1)_e}\}$ by an angle θ_i around the $z'_{(i-1)_e}$-axis. The transformation matrix, defining $\{i\}$ with respect to $\{(i-1)'_e\}$, can be written as

$$T_{(i-1)'_e}^{i} = \begin{bmatrix} c\theta_i & -s\theta_i & 0 & | & 0 \\ s\theta_i & c\theta_i & 0 & | & 0 \\ 0 & 0 & 1 & | & 0 \\ -- & -- & - & - & - \\ 0 & 0 & 0 & | & 1 \end{bmatrix}. \tag{11}$$

Next, the general deformation of the ith link is described by defining a local co-ordinate system $\{x'_i, y'_i, z'_i\}$ at an arbitrary point C on the neutral axis of the ith link. Through sequential transformations, the absolute position vector of any

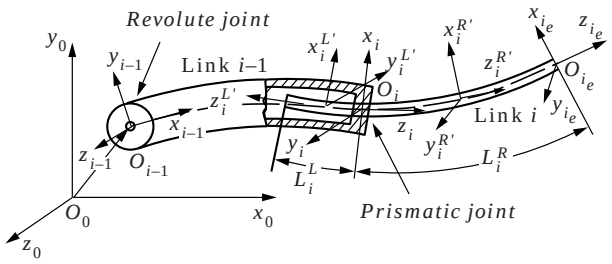

Figure 4. Open-kinematic chain with revolute and prismatic joints.

point B, located on the cross-section of the beam that passes through C, can be expressed as

$$\begin{Bmatrix} \mathbf{r}_B^{\{0\}} \\ -- \\ 1 \end{Bmatrix} = T_0^{i-1} T_{i-1}^{(i-1)_e} T_{(i-1)_e}^{i} \begin{bmatrix} 1 & -\psi_{y_i} & -\psi_{z_i} & | & x_i + u_{a_i} \\ \psi_{y_i} & 1 & 0 & | & v_i \\ \psi_{z_i} & 0 & 1 & | & w_i \\ -- & -- & -- & - & --- \\ 0 & 0 & 0 & | & 1 \end{bmatrix} \begin{Bmatrix} 0 \\ y_i' \\ z_i' \\ -- \\ 1 \end{Bmatrix}. \tag{12}$$

Once again by ignoring Poisson's ratios in the above formulation, one can set $y_{i-1}' = y_{i-1}$, $z_{i-1}' = z_{i-1}$, $y_i' = y_i$ and $z_i' = z_i$.

3.2. CASE II: KINEMATICS OF TWO FLEXIBLE LINKS CONNECTED TO REVOLUTE AND PRISMATIC JOINTS

To expand the implementation of the flexibility matrix, assume that the $(i-1)$th and ith links are connected to a revolute and prismatic joints, respectively (see Figure 4). The length of the portion of the ith link protruding from the $(i-1)$th member can vary with time. Therefore, the ratio of the beam length to its thickness may become less than 10 (thick beam). Thus, the rotary inertia and shear deformation effects must be included in the derivation by implementing the Timoshenko beam theory. Furthermore, the axial geometric shortening effect, resulting from the in-plane and out-of-plane transverse deformations, are also accounted for in the formulation.

The absolute position vector of any point A on the $(i-1)$th member follows directly from equations (9) and (10). To reflect the rotary inertia and shear deformation effects, $\psi_{y_{i-1}}$ and $\psi_{z_{i-1}}$ are expressed as $v_{i-1,x_{i-1}} - \gamma_{xy_{i-1}}$ and $w_{i-1,x_{i-1}} - \gamma_{xz_{i-1}}$, respectively. In addition, the co-ordinate system $\{x_{(i-1)_e'}, y_{(i-1)_e'}, z_{(i-1)_e'}\}$ is defined in a similar fashion as in the previous case. However, the frame, $\{i\}$, is assigned by rotating $\{x_{(i-1)_e'}, y_{(i-1)_e'}, z_{(i-1)_e'}\}$ in a manner complying

with the D–H rules for a prismatic joint. The constant transformation matrix, $T^i_{(i-1)'_e}$, is defined to be

$$T^i_{(i-1)'_e} = \left[\begin{array}{ccc|c} 0 & 0 & 1 & 0 \\ 1 & 0 & 0 & 0 \\ 0 & 1 & 0 & 0 \\ \hline 0 & 0 & 0 & 1 \end{array}\right]. \tag{13}$$

The prismatic joint causes the part of the ith link, protruding from the $(i-1)$th link, to exhibit a different level of vibrations than the portion of the ith member located inside the $(i-1)$th link (see Figure 5). Therefore, these two portions of the ith link have to be modelled separately. A floating co-ordinate system is assigned to each part of the ith link at an arbitrary point on their neutral axes. For the $\{x_i^{R'}, y_i^{R'}, z_i^{R'}\}$ frame, α_1, α_2 and α_3 in equation (3) correspond to $\psi^R_{z_i}$, $\psi^R_{x_i}$ and $-\psi^R_{y_i}$, respectively (see Figures 4 and 5). Note that $\psi^R_{x_i}$ and $\psi^R_{y_i}$ are equal to $u^R_{i,z_i} - \gamma^R_{xz_i}$ and $v^R_{i,z_i} - \gamma^R_{yz_i}$, respectively; whereas, $\psi^R_{z_i}$ is set to zero since the torsional vibration is ignored in this problem. Therefore, the absolute position vector of an arbitrary point B_R, in the $(x_i^{R'}, y_i^{R'})$ plane, can be expressed as (see Figure 4):

$$\{\mathbf{r}^{\{0\}^T}_{B_R}|1\}^T = T^{i-1}_0 T^{(i-1)'_e}_{i-1} T^i_{(i-1)'_e} T^{iR'}_i \{\mathbf{r}^{\{i\}'^T}_{B_R}|1\}^T$$

$$= T^i_0 \left[\begin{array}{ccc|c} 1 & 0 & \psi^R_{x_i} & u^R_i \\ 0 & 1 & \psi^R_{y_i} & v^R_i \\ -\psi^R_{x_i} & -\psi^R_{y_i} & 1 & z_i + w^R_{a_i} \\ \hline 0 & 0 & 0 & 1 \end{array}\right] \left\{\begin{array}{c} x_i^{R'} \\ y_i^{R'} \\ 0 \\ \hline 1 \end{array}\right\}. \tag{14}$$

Note that $x_i^{R'} = x_i$ and $y_i^{R'} = y_i$ since the Poisson's ratios are ignored in this study. z_i represents the translational rigid body degree-of-freedom introduced by the

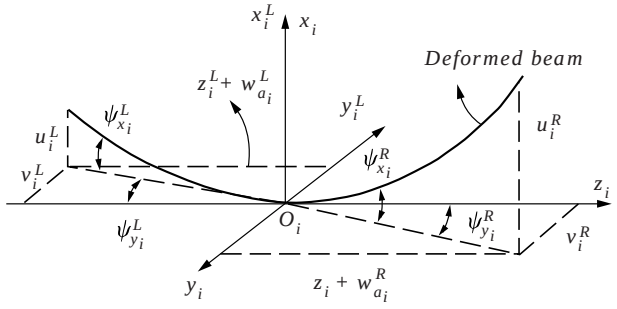

Figure 5. A deformed beam connected to a prismatic joint.

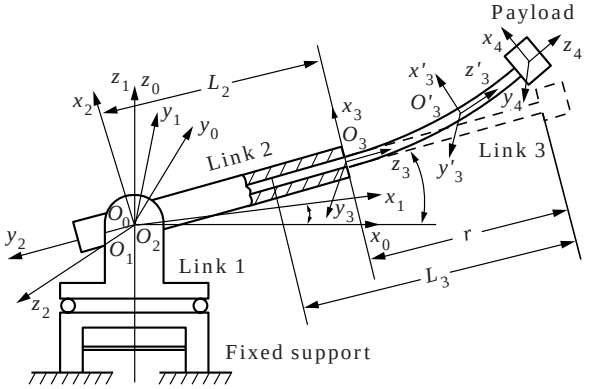

Figure 6. Schematic of the flexible spherical robotic manipulator.

prismatic joint. Next, the absolute position vector of an arbitrary point B_L, in the $(x_i^{L\prime}, y_i^{L\prime})$ plane, is defined to be

$$\{\mathbf{r}_{B_L}^{\{0\}^T}|1\}^T = T_0^{i-1}T_{i-1}^{(i-1)'_e}T_{(i-1)'_e}^{i}T_i^{i_L}T_{i_L}^{i_L\prime}\{\mathbf{r}_{B_L}^{\{i\}'^T}|1\}^T$$

$$= T_0^i \begin{bmatrix} 1 & 0 & \psi_{x_i}^L & | & u_i^L(z_i^L, t) \\ 0 & -1 & -\psi_{y_i}^L & | & -v_i^L(z_i^L, t) \\ \psi_{x_i}^L & \psi_{y_i}^L & -1 & | & -z_i^L - w_{a_i}^L(z_i^L, t) \\ - & - & - & - & --- \\ 0 & 0 & 0 & | & 1 \end{bmatrix} \begin{Bmatrix} x_i^{L\prime} \\ y_i^{L\prime} \\ 0 \\ -- \\ 1 \end{Bmatrix}. \quad (15)$$

It should be emphasized that $\psi_{x_i}^L$ and $\psi_{y_i}^L$ represent $u_{i,z_i}^L - \gamma_{xz_i}^L$ and $v_{i,z_i}^L - \gamma_{yz_i}^L$ rotations around the y_i^L and $-x_i^L$ axes, respectively (see Figures 4 and 5). Again, x_i^L and y_i^L are equal to x_i and $-y_i$, respectively. z_i^L corresponding to the portion of the ith link, located inside the $(i-1)$th link, must satisfy $0 \leqslant z_i^L \leqslant L_i^L$.

One can easily verify that the D–H formulation for the rigid body configuration of the kinematic chain can be directly recovered from the above derivation by simply deleting all the structural flexibility terms.

4. DYNAMIC MODELLING OF A FLEXIBLE SPHERICAL ROBOTIC MANIPULATOR

The current transformation matrix is used herein to systematically derive the equations of motion for a spherical robotic manipulator (see Figure 6). The formulation takes into consideration the torsional along with the transverse deformations of the protruding part of the third link. The first two links of the robot are treated as rigid bodies. They are connected to revolute joints which employ harmonic drives. The third link is connected to a prismatic joint whose indirect drive is comprised of a ball bearing leadscrew. Since the length of the protruding part of the third link varies with the arm geometric configuration then

the ratio of the length to the width of the compliant portion of the third link is kept larger than 10. Hence, the shear deformation can be ignored and the structural deformation can be adequately formulated by the Euler–Bernoulli beam theory. In addition, the longitudinal deformation is neglected, since the compliant beam is much stiffer in the axial direction than in flexure. Moreover, the viscous damping at the joints are included in the formulation.

An inertial co-ordinate system, having its origin at O_0 and its z_0-axis coinciding with the axis of rotation of the base joint, is first assigned (see Figure 6). Then, a non-inertial co-ordinate system is rigidly attached to each of the first and second links according to the D–H rules. Moreover, a co-ordinate system $\{x_3, y_3, z_3\}$ is attached to the end of the second rather than the third link. This slight modification of the D–H rules is designed to systematically handle the kinematics of a compliant link that is connected to a prismatic joint. The z_3-axis is assigned to line up with the neutral axis of the third link. Then, a floating co-ordinate system, $\{x_3', y_3', z_3'\}$, is assigned such that its z_3'-axis remains tangent to the neutral axis of the compliant portion of the third link. Finally, the dynamics of the payload are represented with respect to the $\{x_4, y_4, z_4\}$ frame which is attached to the free-end of the third link.

The locations and orientations of the first three frames are defined with respect to the inertial co-ordinate system according to the following 4×4 matrices:

$$T_0^1 = \left[\begin{array}{ccc|c} c\theta_1 & -s\theta_1 & 0 & 0 \\ s\theta_1 & c\theta_1 & 0 & 0 \\ 0 & 0 & 1 & 0 \\ \hline 0 & 0 & 0 & 1 \end{array}\right],$$

$$T_0^2 = T_0^1 T_1^2 = \left[\begin{array}{ccc|c} -c\theta_1 s\theta_2 & -c\theta_1 c\theta_2 & s\theta_1 & 0 \\ -s\theta_1 s\theta_2 & -s\theta_1 c\theta_2 & -c\theta_1 & 0 \\ c\theta_2 & -s\theta_2 & 0 & 0 \\ \hline 0 & 0 & 0 & 1 \end{array}\right], \tag{16}$$

$$T_0^3 = T_0^1 T_1^2 T_2^3 = \left[\begin{array}{ccc|c} -c\theta_1 s\theta_2 & s\theta_1 & c\theta_1 c\theta_2 & L_2 c\theta_1 c\theta_2 \\ -s\theta_1 s\theta_2 & -c\theta_1 & s\theta_1 c\theta_2 & L_2 s\theta_1 c\theta_2 \\ c\theta_2 & 0 & s\theta_2 & L_2 s\theta_2 \\ \hline 0 & 0 & 0 & 1 \end{array}\right].$$

The structural flexibility matrix, which describes the deformations at an arbitrary point on the neutral axis of the protruding part of the third link, is expressed as

$$T_3^{3\prime} = \begin{bmatrix} 1 & -\psi_{z_3} & \psi_{x_3} & | & u_3 \\ \psi_{z_3} & 1 & \psi_{y_3} & | & v_3 \\ -\psi_{x_3} & -\psi_{y_3} & 1 & | & z_3 + w_3 \\ -- & -- & -- & - & -- \\ 0 & 0 & 0 & | & 1 \end{bmatrix}. \tag{17}$$

Since the rotary inertia and shear deformations are ignored then ψ_{x_3} and ψ_{y_3} become equal to u_{3,z_3} and v_{3,z_3}, respectively. In addition, ψ_{z_3} represents the torsional vibration of the third link, ϕ, around z_3-axis. It should be mentioned that the location and orientation of $\{x_4, y_4, z_4\}$ with respect to $\{x_3, y_3, z_3\}$ can be readily obtained by evaluating $T_3^{3\prime}$ at $z_3 = r$.

The extended absolute position vector of an arbitrary point, A, on the ith link can be determined from

$$\{\mathbf{r}_A^{\{0\}^T}|1\}^T = T_0^{i\prime}\{\mathbf{r}_A^{\{i\}^{\prime T}}|1\}^T, \tag{18}$$

whose time derivative is given by

$$\{\dot{\mathbf{r}}_A^{\{0\}^T}|1\}^T = \dot{T}_0^{i\prime}\{\mathbf{r}_A^{\{i\}^{\prime T}}|1\}^T + T_0^{i\prime}\{\dot{\mathbf{r}}_A^{\{i\}^{\prime T}}|1\}^T. \tag{19}$$

Note that in the case of a rigid ith link, the prime should be ignored in the above formulation.

The structural flexibility terms, u_3, v_3 and ϕ, are approximated by using the assumed modes method. The admissible functions are selected to be the eigenfunctions of the torsional, in-plane and out-of-plane transverse deformations of a clamped–free beam. In addition, it is assumed that u_3, v_3 and ϕ are dominated by the first two elastic modes. This is because higher modes are unlikely to be excited due to the limited bandwidth of the joint actuators. Consequently, one can write

$$u_3(z_3, t) = \sum_{i=1}^{2} \Phi_i(z_3) u_{3_i}(t), \qquad v_3(z_3, t) = \sum_{i=1}^{2} \Phi_i(z_3) v_{3_i}(t),$$

$$\phi(z_3, t) = \sum_{i=1}^{2} \Psi_i(z_3)\phi_i(t). \tag{20}$$

It should be pointed out that the elastic modes are derived based on the simple beam theory which do not account for the axial geometric shortening effect of the beam. The latter is required to preserve the inextensional characteristic of a beam of which one of its extremities is free from any displacement constraint. To correct for the deficient mode shapes, the axial elastic displacement, w_3, in $T_3^{3\prime}$ is defined to be the axial geometric shortening of the neutral axis, w_{3a}, induced by the transverse deformations. This effect, which is not captured by the mode shapes

that are used in the discretization of the structural flexibility terms, can be described as follows:

$$w_{3a}(z_3, t) = -\frac{1}{2}\int_0^{z_3}\left[\left(\frac{\partial u_3}{\partial \alpha}\right)^2 + \left(\frac{\partial v_3}{\partial \alpha}\right)^2\right] \mathrm{d}\alpha. \tag{21}$$

Now that the expressions of the position and velocity vectors are fully defined, the kinetic energy term can be derived. Since the first and second links undergo fixed point rotations, then their kinetic energy expressions can be written in the form

$$T_1 = \frac{1}{2}\sum_{i=1}^{2} \boldsymbol{\omega}_i^{\{i\}^T} H_i \boldsymbol{\omega}_i^{\{i\}}, \tag{22}$$

where $\boldsymbol{\omega}_1^{\{1\}} = \dot{\theta}_1 \mathbf{k}_1$ and $\boldsymbol{\omega}_2^{\{2\}} = \dot{\theta}_1 \cos\theta_2 i_2 - \dot{\theta}_1 \sin\theta_2 \mathbf{j}_2 + \dot{\theta}_2 \mathbf{k}_2$. The payload and the portion of the third link, located inside the second link, are treated as rigid bodies undergoing translations and rotations. Their kinetic energy expressions can be determined from

$$T_2 = \frac{1}{2}\left(\boldsymbol{\omega}_{3r}^{\{3\}^T} H_{3r} \boldsymbol{\omega}_{3r}^{\{3\}} + \boldsymbol{\omega}_6^{\{4\}^T} H_6 \boldsymbol{\omega}_6^{\{4\}} + \sum_{i=3r\&6} m_i \dot{\mathbf{r}}_{imc}^{\{0\}} \cdot \dot{\mathbf{r}}_{imc}^{\{0\}}\right), \tag{23}$$

where $\boldsymbol{\omega}_{3r}^{\{3\}} = \dot{\theta}_1 \cos\theta_2 \mathbf{i}_3 + \dot{\theta}_2 \mathbf{j}_3 + \dot{\theta}_1 \sin\theta_2 \mathbf{k}_3$. Since the payload is assumed to be rigidly attached to the free-end of the third link, its angular velocity vector becomes

$$\boldsymbol{\omega}_6^{\{4\}} = (\boldsymbol{\omega}_{3f}^{\{4\}})_{z_3 = r} = \begin{Bmatrix} \dot{\theta}_1 \cos\theta_2 + \psi_{z_3}\dot{\theta}_2 - \psi_{x_3}\dot{\theta}_1 \sin\theta_2 - \dot{\psi}_{y_3} \\ \dot{\theta}_2 - \psi_{z_3}\dot{\theta}_1 \cos\theta_2 - \psi_{y_3}\dot{\theta}_1 \sin\theta_2 + \dot{\psi}_{x_3} \\ \dot{\theta}_1 \sin\theta_2 + \psi_{x_3}\dot{\theta}_1 \cos\theta_2 + \psi_{y_3}\dot{\theta}_2 + \dot{\psi}_{z_3} \end{Bmatrix}_{z_3 = r}. \tag{24}$$

The kinetic energy expressions of the compliant portion of the third link along with the ball-bearing leadscrew assembly and the gripper can be determined from

$$T_3 = \frac{1}{2}\int_{m_{3f}} \dot{\mathbf{r}}_{3f}^{\{0\}} \cdot \dot{\mathbf{r}}_{3f}^{\{0\}} \, \mathrm{d}m_{3f} + \frac{1}{2}\sum_{i=4}^{5} m_i \dot{\mathbf{r}}_i^{\{0\}} \cdot \dot{\mathbf{r}}_i^{\{0\}}. \tag{25}$$

The total kinetic energy of the robotic manipulator can then be obtained by adding the above expressions for T_1 to T_3.

Next, the potential energy of the robot arm is expressed as

$$V = \frac{1}{2}\int_0^r \{EI[u_{3,z_3z_3}^2 + v_{3,z_3z_3}^2] + GJ\phi^2\} \, \mathrm{d}z_3 + \int_0^r \rho A_3 (\mathbf{r}_{3f}^{\{0\}} \cdot g\mathbf{k}_0) \, \mathrm{d}z_3$$

$$+ \sum_i g\mathbf{k}_0 \cdot m_i \mathbf{r}_{imc}^{\{0\}}, \qquad i = 1, 2, 3r, 4, 5 \text{ and } 6, \tag{26}$$

where the datum line is considered to coincide with the x_0-axis.

TABLE 1

Numerical values for the robot parameters

Length of the second link (L_2)	0·533 m
Length of the third link (L_3)	0·77 m
Diameter of the third link (D_3)	0·0127 m
Mass moment of inertia of the first link around the z_0-axis	0·259 kg · m^2
Mass moment of inertia of the second link around the x_2, y_2 and z_2 axes, respectively	0·401, 0·015, 0·408 kg · m^2
Mass of the second link (m_2)	9·424 kg
Mass of the end-effector (m_e)	0·127 kg
Mass of the payload (m_p)	0·213 kg

5. DIGITAL SIMULATION RESULTS

A linear quadratic regulator with an integral action (LQI) controller is implemented to perform point-to-point (PTP) maneuvers of the arm. The controller is designed based on a linearized version of the rigid body equations of motion of the robotic manipulator. The reduced state vector along with the controller weighting matrices are defined to be

$$\mathbf{x}_r^T = \left[\theta_1, \theta_2, r, \dot{\theta}_1, \dot{\theta}_2, \dot{r}, \int (\theta_1 - \theta_{1_d})\,\mathrm{d}t, \int (\theta_2 - \theta_{2_d})\,\mathrm{d}t, \int (r - r_d)\,\mathrm{d}t\right],$$

$$Q_r = \mathrm{diag}\,[0{\cdot}1, 0{\cdot}1, 0{\cdot}1, 0, 0, 0, 10, 10, 10], \qquad R_r = \mathrm{diag}\,[1, 1, 1] \times 10^{-6}. \quad (32)$$

The LQI controller is then applied on the full non-linear model of the robotic manipulator whose geometric dimensions are listed in Table 1. The full state vector is given by $\tilde{\mathbf{x}}^T = [\mathbf{q}^T, \dot{\mathbf{q}}^T, \int (\theta_1 - \theta_{1_d})\,\mathrm{d}t, \int (\theta_2 - \theta_{2_d})\,\mathrm{d}t, \int (r - r_d)\,\mathrm{d}t]$. The arm is assigned a PTP task with the initial and final states defined to be $\tilde{\mathbf{x}}_0^T = \{0\ \ 0\ \ 0{\cdot}2 \mid 0_{1\times 18}\}$ and $\tilde{\mathbf{x}}_F^T = \{90^\circ\ \ 60^\circ\ \ 0{\cdot}6 \mid 0_{1\times 18}\}$, respectively. Initially, the payload is considered to be grasped at its mass center by the gripper. The oscillations of the in-plane and out-of-plane transverse deformations at the end-effector are shown in Figures 7 and 8, respectively. The interaction between

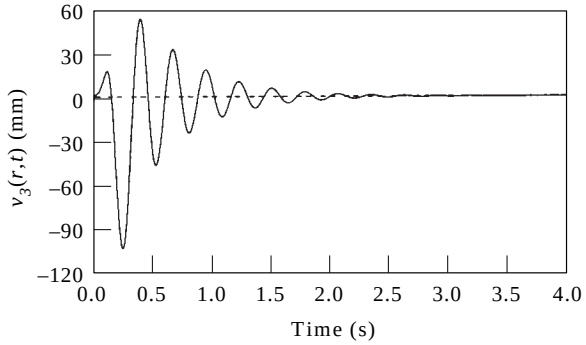

Figure 7. In-plane transverse deformation at the end-effector generated while holding the payload at its mass center.

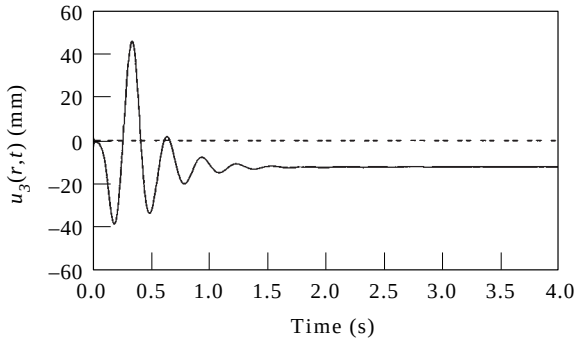

Figure 8. Out-of-plane transverse deformation at the end-effector generated while holding the payload at its mass center.

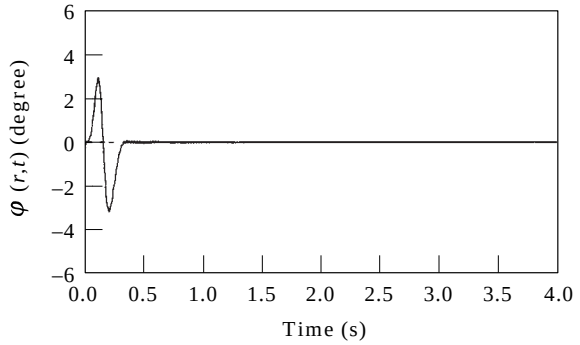

Figure 9. Torsional vibration at the end-effector generated while holding the payload at its mass center.

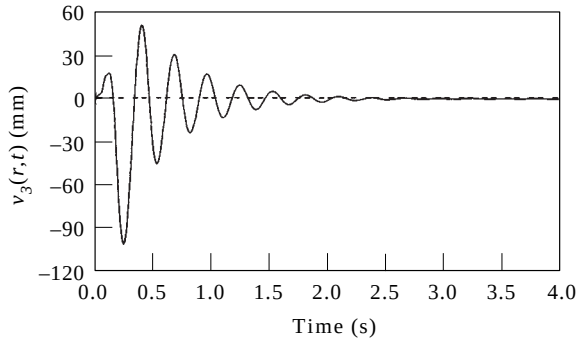

Figure 10. In-plane transverse deformation at the end-effector generated with an offsetted payload.

the torsional vibration and the rigid body motion of the arm is clearly manifested in Figure 9. The initial excitation of the torsional vibration is induced by the inertial forces during the transient period of the arm response. Furthermore, the steady state response of ϕ is virtually undisturbed because the torsional and transverse deformations of the third link are decoupled whenever the payload is held by its mass center.

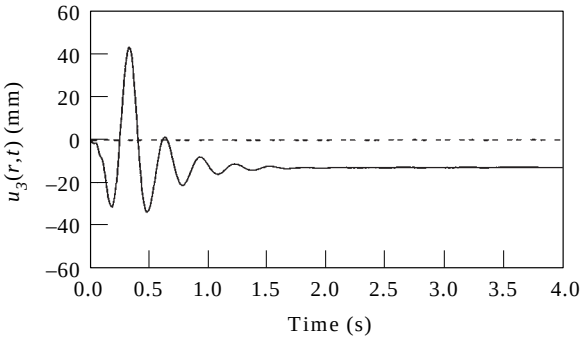

Figure 11. Out-of-plane transverse deformation at the end-effector generated with an offsetted payload.

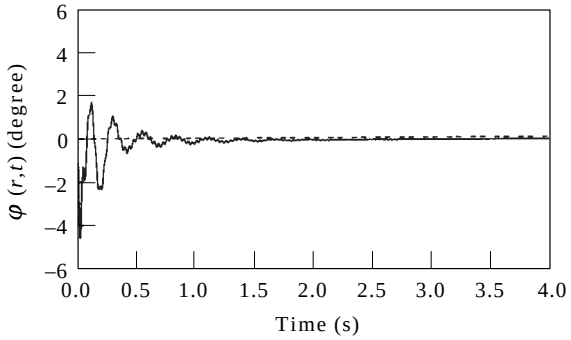

Figure 12. Torsional vibration at the end-effector generated with an offsetted payload.

Next, the same PTP maneuver is repeated while grabbing the payload in such a manner that its mass center co-ordinates are located at $x_4 = -0{\cdot}0707m$, $y_4 = -0{\cdot}0707m$ and $z_4 = 0m$ with respect to the gripper. Figures 10 and 11 reveal slightly smaller amplitudes for the transverse deformations than their counterparts from Figures 7 and 8 during the transient phase of the arm response. Furthermore, the low frequency component in the ϕ plot manifests the interaction between the transverse and torsional vibrations of the third link which is triggered by the offset of the payload mass center with respect to the end-effector (see Figure 12). It should also be mentioned that the non-zero steady state values of the torsional vibration, ϕ, and the in-plane transverse deformation, v_3, are caused by the static torque and force arising from the offset of the payload.

6. SUMMARY AND CONCLUSIONS

The structural flexibility matrix is intended to complement the D–H transformation matrix in the development of a conceptually straightforward modelling approach that exploits the inherent serial characteristic of compliant open-kinematic chains. The structural flexibility matrices, currently available in the literature, are derived based on a body fixed co-ordinate system which limits their application to articulated kinematic chains. The present formulation departs

from previous work by deriving the structural flexibility matrix with respect to a floating co-ordinate system. As a result, the formulation can now describe deformations of beams that are connected to either prismatic or revolute joints. In addition, the flexibility matrix, developed herein, can represent the torsional, longitudinal, in-plane and out-of-plane transverse deflections along with their axial geometric shortening, rotary inertia and shear deformation effects.

The versatility of the current formulation is demonstrated by implementing the D–H and flexibility matrices to solve forward kinematic problems of flexible manipulators with revolute and prismatic joints. Furthermore, the proposed flexibility matrix is used in the development of a dynamic model for a spherical robotic manipulator. This task has a dual purpose. First, it demonstrates how the flexibility matrix can be implemented in a systematic approach for deriving the equations of motion of an open-kinematic chain that take into account the axial geometric shortening, the torsional vibration, the in-plane and out-of-plane transverse deformations of the compliant link. Second, the inclusion of the torsional vibration in addition to the transverse deformations in the equations of motion has served to broaden the scope of previous research work, done on modelling open-kinematic chains, to address dynamic problems that are not limited to the positioning but also concerned with the orientation of rigid body payloads as they are being manipulated by multi-link robotic manipulators. The digital simulation results have revealed the interaction between the torsional vibration and the rigid body motion of the arm. Moreover, they have demonstrated a strong coupling effect between the torsional vibration and the transverse deformations of the arm whenever the payload is not grasped at its mass center by the gripper.

REFERENCES

1. D. A. Turcic and A. Midha 1984 *ASME Journal of Dynamic Systems, Measurement, and Control* **106**, 243–248. Generalized equations of motion for the dynamic analysis of elastic mechanism systems.
2. N. G. Chalhoub and A. G. Ulsoy 1986 *ASME Journal of Dynamic Systems, Measurement and Control* **108**, 119–126. Dynamic simulation of a leadscrew driven flexible robot arm and controller.
3. P. B. Usoro, R. Nadira and S. S. Mahil 1986 *ASME Journal of Dynamic Systems, Measurement, and Control* **108**, 198–205. A finite element/Lagrange approach to modeling lightweight flexible manipulators.
4. W. H. Sunada and S. Dubowsky 1983 *ASME Journal of Mechanisms, Transmissions, and Automation in Design* **105**, 42–51. On the dynamic analysis and behavior of industrial robotic manipulators with elastic members.
5. J. Denavit and R. S. Hartenberg 1955 *ASME Journal of Applied Mechanics* **22**, 215–221. A kinematic notation for lower-pair mechanisms based on matrices.
6. W. J. Book 1984 *International Journal of Robotics Research* **3**, 87–101. Recursive Lagrangian dynamics of flexible manipulator arms.
7. R. P. Judd and D. R. Falkenburg 1985 *IEEE Transactions on Automatic Control* **AC-30**, 499–502. Dynamics of nonrigid articulated robot linkages.
8. F. Matsuno and Y. Sakawa 1990 *Journal of Robotic Systems* **7**, 575–597. A simple model of flexible manipulators with six axes and vibration control by using accelerometers.

9. C. J. Li and T. S. Sankar 1992 *Journal of Robotic Systems* **9**, 861–891. A systematic method of dynamics for flexible robot manipulators.
10. L. Chen 1995 *PhD Thesis*, *Wayne State University*, *Detroit*. Dynamic modeling and active control of the torsional and transverse vibrations of flexible spherical robotic manipulators.
11. S. P. Bhat and D. K. Miu 1990 *ASME Journal of Dynamic Systems*, *Measurement*, *and Control* **112**, 667–674. Precise point-to-point positioning control of flexible structures.
12. A. Azhdari, N. G. Chalhoub and F. Gordaninejad 1991 *Journal of Nonlinear Dynamics* **2**, 171–186. Dynamic modeling of a revolute-prismatic flexible robot arm fabricated from advanced composite materials.
13. S. Cetinkunt and S. Wu 1991 *International Journal of Control* **53**, 311–333. Output predictive adaptive control of a single-link flexible arm.
14. Y. K. Kim and J. Gibson 1991 *IEEE Transactions on Robotics and Automation* **7**, 818–827. A variable-order adaptive controller for a manipulator with a sliding flexible link.
15. N. G. Chalhoub and X. Zhang 1993 *ASME Journal of Dynamic Systems*, *Measurement and Control* **115**, 658–666. Reduction of the end effector sensitivity to the structural deflections of a single flexible link: theoretical and experimental results.
16. Y. Sakawa and Z. H. Luo 1989 *IEEE Transactions on Automatic Control* **34**, 970–977. Modeling and control of coupled bending and torsional vibrations of flexible beams.
17. S. Timoshenko, D. H. Young and W. J. R. Weaver 1974 *Vibration Problems in Engineering*. New York: John Wiley & Sons; fourth edition.
18. J. J. D'azzo and C. H. Houpis 1988 *Linear Control System Analysis and Design*: *Conventional and Modern*. New York: McGraw-Hill; third edition.

APPENDIX: NOMENCLATURE

A_3	cross-sectional area of the third link
EI	flexural rigidity of the third link
f_3	control force at the prismatic joint
$\mathbf{F}(\mathbf{q}, \dot{\mathbf{q}})$	vector including all inertial forces, stiffness and damping terms
G, g	shearing modulus of elasticity and gravitational acceleration, respectively
H_i	inertia tensor of the ith component defined with respect to the ith frame
J	polar moment of inertia of the cross-sectional area of the third link with respect to the z_3-axis
L_i	length of the ith link
$M(\mathbf{q})$	inertia tensor of the entire robotic manipulator
m_e, m_i, m_p	mass of the end-effector, the ith member and the payload, respectively
$\mathbf{Q}^{NC}$	non-conservative generalized force vector
r	length of the protruding part of the third link from the second link
$\mathbf{r}_A^{\{i\}}$	position vector of an arbitrary point A with respect to the ith frame
$\mathbf{r}_{i_{mc}}^{\{0\}}$	position vector of the mass center of the ith component of the robot arm with respect to the inertial frame
u, v, w	elastic displacements of an arbitrary point on the neutral axis along the x, y and z axes, respectively
(x_i, y_i, z_i)	local co-ordinates of an arbitrary point in the undeformed configuration of the ith link
γ_{xy}, γ_{xz}	shear deformation in the (x, y) and (x, z) planes, respectively
θ_i	rigid body angular displacement of the ith link relative to the $(i-1)$th link
ρ	density of the third link
τ_i	control torque at the ith joint
$\psi_{x_3}, \psi_{y_3}, \psi_{z_3}$	rotations around the y_3, $-x_3$ and z_3 axes, respectively
ϕ	torsional deformation of the third link around the z_3-axis